https://doi.org/10.5194/egusphere-2023-1774
Preprint. Discussion started: 17 October 2023

Rapid Iodine Oxoacids Nucleation Enhanced by Dimethylamine in Broad Marine Regions

Haotian Zu[1], Biwu Chu[2], Yiqun Lu[3], Ling Liu[1*], Xiuhui Zhang[1*]

[1]Key Laboratory of Cluster Science, Ministry of Education of China, School of Chemistry and Chemical Engineering, Beijing Institute of Technology, Beijing 100081, China

[2]State Key Joint Laboratory of Environment Simulation and Pollution Control, Research Center for Eco-Environmental Sciences, Chinese Academy of Sciences, Beijing 100085, China

[3]State Environmental Protection Key Laboratory of Formation and Prevention of Urban Air Pollution Complex, Shanghai Academy of Environmental Sciences, Shanghai 200233, China

Correspondence to: Ling Liu (lingliu@bit.edu.cn) and Xiuhui Zhang (zhangxiuhui@bit.edu.cn)

Abstract. Recent experiment (He et al, 2021, *Science*) revealed a vital nucleation process of iodic acid (HIO_3) and iodous acid (HIO_2) under the marine boundary layer conditions. However, HIO_3-HIO_2 nucleation cannot effectively derive the observed rapid new particle formation (NPF) in broad marine regions. Dimethylamine (DMA) is a promising basic precursor to enhance nucleation considering its strong ability to stabilize acidic clusters and the wide distribution in marine atmosphere, while its role in HIO_3-HIO_2 nucleation remains unrevealed. Hence, a method combining quantum chemical calculations and Atmospheric Cluster Dynamics Code (ACDC) simulations was utilized to study the HIO_3-HIO_2-DMA nucleation process. We found that DMA can compete with HIO_2 to accept the proton from HIO_3 as a basic precursor in the most stable configurations of HIO_3-HIO_2-DMA clusters. DMA can significantly enhance the cluster formation rates of HIO_3-HIO_2 kinetically for more than 10^3-fold in regions with abundant amine and scarce iodine based on combined factors of high nucleation ability and high concentration of DMA. Furthermore, the iodine oxoacids nucleation enhanced by DMA may explain the sources of rapid NPF events under different conditions corresponding to multiple ocean regions, which can provide important inspirations to understand the frequent and intensive NPF events in broad marine regions.

1 Introduction

Atmospheric aerosols, the intricate suspension formed by fine particles in the atmosphere, exert far-reaching influences on global climate (Haywood and Boucher, 2000; Murphy and Ravishankara, 2018; Lee et al., 2019), radiation balance (Haywood and Boucher, 2000), and human health (Pope and Dockery, 2006; Gong et al., 2014). Given the vast expanses of the ocean, marine aerosols play an indispensable role in the global aerosol system (O'dowd and De Leeuw, 2007). A significant source of atmospheric aerosols on the world-wide scale is the process of new particle formation (NPF), encompassing nucleation and subsequent growth (Zhang, 2010). The initial nucleation is identified as the key process of NPF events. Therefore, understanding the NPF nucleation mechanism under marine atmospheric conditions is vital for comprehending the behavior of marine aerosols (Zhang et al., 2012; Kalivitis et al., 2015).

Iodine species are originated from biological emissions of marine macroalgae (O'dowd et al., 2002a; O'dowd et al., 2002c; O'dowd et al., 2002b; Zhang et al., 2012) and thought to be important precursors of the frequent NPF events in mid-latitudes coastal as well as high-latitudes polar regions (Hoffmann et al., 2001; Ehn et al., 2010; Mcfiggans et al., 2010; Mahajan et al., 2011; Baccarini et al., 2020). Several studies have consistently highlighted the pivotal role of iodic acid (HIO_3) in marine nucleation processes (Sipila et al., 2016; Yu et al., 2019; Baccarini et al., 2020; Rong et al., 2020; Xia et al., 2020; He et al., 2021). Molecular-level observations conducted at the Mace Head coastal station in Ireland have provided evidence that the nucleation process is predominantly driven by HIO_3 with high concentration (Sipila et al., 2016). Iodous acid (HIO_2) was also detected in both gas and particle phases during the NPF events together with the HIO_3 (Sipila et al.,

https://doi.org/10.5194/egusphere-2023-1774
Preprint. Discussion started: 17 October 2023

2016; Yu et al., 2019). Recently, HIO_2 has been confirmed to play an important role in stabilizing the neutral HIO_3 clusters in the Cosmics Leaving OUtdoor Droplets (CLOUD) chamber in European Organization for Nuclear Research (CERN) (He et al., 2021). This was found to be concerned with the alkaline property of HIO_2 in HIO_3-HIO_2 clusters by subsequent theoretical studies (Zhang et al., 2022a; Liu et al., 2023). Though binary nucleation of HIO_3-HIO_2 has been widely concerned in the oceanic atmosphere, only the HIO_3-HIO_2 nucleation cannot explain the rapid NPF in broad marine areas (Ma et al., 2023), which indicates that other nucleation precursors may be involved.

In addition to iodine species, dimethylamine (DMA) is also a common nucleation precursor in the oceanic atmosphere (Facchini et al., 2008). DMA can originate from plankton and bacteria in seawater (Muller et al., 2009; Hu et al., 2015; Chen et al., 2021). Moreover, ice-influenced ocean may also be important sources of DMA (Dall'osto et al., 2017; Dall'osto et al., 2019). Hence, DMA is widely distributed and abundant under the different oceanic atmospheric conditions, displaying a spatial distribution remarkably akin to that of iodine species in mid-latitudes coastal and high-latitudes polar regions (Vanneste et al., 1987; Gronberg et al., 1992; Gibb et al., 1999; Quelever et al., 2022). Previous studies have shown that DMA has strong base-stabilization effect on the sulfuric acid (SA) nucleation process (Almeida et al., 2013; Yao et al., 2018), because DMA possesses relatively strong basicity. Therefore, DMA also has potential to participate in and facilitate the nucleation process of HIO_3-HIO_2 through additional acid-base interactions. However, former studies did not pay enough attention to DMA's impact on the HIO_3-HIO_2 nucleation in broad marine regions, and the ternary nucleation mechanism of HIO_3-HIO_2-DMA remains to be disclosed.

In the present study, the nucleation mechanism of HIO_3-HIO_2 enhanced by DMA under atmospheric conditions of different marine regions (mid-latitudes coastal and high-latitudes polar regions) were studied by a method combining quantum chemical calculation and Atmospheric Cluster Dynamics Code (ACDC) model. The simulated system contains $(HIO_3)_x\cdot(HIO_2)_y\cdot(DMA)_z$ ($1 \le x + y + z \le 5$; $x + y \ge z$) clusters. The largest clusters with a mobility diameter (Almeida et al., 2013) up to 1.2 nm in the size range of nucleation clusters (Zhang et al., 2012) are stable enough to resist evaporation at the studied temperature, and clusters with more DMA molecules ($x + y < z$) are usually unstable. This study aims to reveal the potential role of DMA in the HIO_3-HIO_2 nucleation and help to better understand the intensive NPF events in broad marine regions.

2 Method

2.1 Quantum chemical calculations

The HIO_3-HIO_2-DMA system is composed of ternary clusters (HIO_3-HIO_2-DMA), binary clusters (HIO_3-HIO_2, HIO_3-DMA, HIO_2-DMA) and the pure HIO_x (x = 2, 3) clusters. The most stable configuration of HIO_3-HIO_2-DMA ternary clusters and HIO_2-DMA binary clusters were proposed in this study for the first time. Additionally, the structures of HIO_3-HIO_2/DMA clusters and pure-HIO_x (x = 2, 3) clusters presented in this work were adopted from the stable configurations with the lowest Gibbs free energy of formation in previous studies (Rong et al., 2020; Ning et al., 2022; Zhang et al., 2022b; Liu et al., 2023) at the same level of theory. A multi-step searching progress that can systematically screen the structures of clusters was adopted in this research. Firstly, the ABCluster program (Zhang and Dolg, 2015) was performed to generate up to 120000 initial isomer structures using the artificial bee algorithm. The universal force field (UFF) (Rappé et al., 1992) was chosen to select up to 1000 structures with lower energies from the initial isomer structures. Secondly, 1000 structures for each cluster were pre-optimized by the PM7 semi-empirical method (Stewart, 2013) with Mopac 2016 program (Stewart, 2016) to choose 100 structures with relatively low energies. Then 100 structures were optimized at the ωB97X-D/6-31+G* (for H, C, N and O atoms) + Lanl2DZ (for I atom) level of theory (Yang et al., 2009; Elm, 2013) to find out 10 relatively stable structures of all. Finally, 10 stable structures were reoptimized at the ωB97X-D/6-311++G (3df, 3pd) (for H, C, N and O atoms) + aug-cc-pVTZ-PP (for I atom) level of theory (Frisch et al., 1984; Peterson, 2003; Chai and Head-Gordon, 2008; Elm and Kristensen, 2017) together with the calculations of vibrational frequencies. All quantum chemical calculations were performed using the Gaussian 09 package (Frisch et al., 2009) to identify the most stable conformations of each cluster. Afterwards, the single-point energy correction was carried out by the RI-CC2/aug-cc-pVTZ (for H, C, N and O atoms) +

https://doi.org/10.5194/egusphere-2023-1774
Preprint. Discussion started: 17 October 2023

aug-cc-pVTZ-PP with ECP28MDF (for I atom) using the Turbomole program (Ahlrichs, 1989), because of the good agreement between simulated results (e.g., the cluster formation rates) at the this theoretical level with the experimental results or field measurements through a random cancellation of errors (Almeida et al., 2013; Kuerten et al., 2018; Lu et al., 2020).

In the present study, the Gibbs free energy of formation (ΔG, kcal mol^{-1}) of clusters was calculated as:

$$\Delta G = \Delta E_{\mathrm{RI-CC2}} + \Delta G_{\mathrm{thermal}}^{\omega\mathrm{B97X-D}}$$

where $\Delta E_{\mathrm{RI-CC2}}$ is the electronic contribution obtained at the RI-CC2/aug-cc-pVTZ (for H, C, N and O atoms) + aug-cc-pVTZ-PP with ECP28MDF (for I atom) level of theory, and $\Delta G_{\mathrm{thermal}}^{\omega\mathrm{B97X-D}}$ is the thermal contribution calculated at the ωB97X-D/6-311++G(3df,3pd) (for H, C, N and O atoms) + aug-cc-pVTZ-PP with ECP28MDF (for I atom) level of theory.

2.2 Atmospheric Cluster Dynamics Code (ACDC) simulations

In order to investigate the effect of DMA on HIO_3-HIO_2 nucleation in marine areas, a series of ACDC simulations (Mcgrath et al., 2012) were performed under atmospheric conditions corresponding to mid-latitudes coastal and high-latitudes polar regions. By solving the birth-death equation, the ACDC simulations can obtain the cluster formation rates and formation pathways of clusters using the MATLAB program (Shampine and Reichelt, 1997). The birth-death equation can be written as follows:

$$\frac{dc_i}{dt} = \frac{1}{2}\sum_{j<i}\beta_{j,(i-j)}c_j c_{i-j} + \sum_j \gamma_{(i+j)\to i}c_{i+j} - \sum_j \beta_{i,j}c_i c_j - \frac{1}{2}\sum_{j<i}\gamma_{i\to j}c_i + Q_i - S_i$$

where c_i is the concentration of cluster i, $\beta_{i,j}$ is the collision coefficient between cluster i and cluster j, $\gamma_{(i+j)\to i}$ is the evaporation coefficient of the cluster ($i+j$) evaporating into cluster i and cluster j, Q_i is the external source term of cluster i, and S_i is the potential sink term for cluster i.

The collision coefficient $\beta_{i,j}$ can be written as:

$$\beta_{i,j} = \left(\frac{3}{4\pi}\right)^{\frac{1}{6}}\left(\frac{6k_{\mathrm{B}}T}{m_i} + \frac{6k_{\mathrm{B}}T}{m_j}\right)^{\frac{1}{2}}\left(V_i^{\frac{1}{3}} + V_j^{\frac{1}{3}}\right)^2$$

where k_{B} is the Boltzmann constant, T is the temperature, m_i is the mass of cluster i, and V_i is the van der Waals volume of cluster i, which is calculated by the improved Marching Tetrahedra (MT) approach (Lu and Chen, 2012a) using Multiwfn 3.7 program (Lu and Chen, 2012b).

The evaporation coefficient $\gamma_{(i+j)\to i}$ of the cluster was obtained from the collision coefficient and the specific balance between cluster formation via the collision and cluster loss via the evaporation:

$$\gamma_{(i+j)\to i} = \beta_{i,j}c_{\mathrm{ref}}\exp\left(\frac{\Delta G_{i+j} - \Delta G_i - \Delta G_j}{k_{\mathrm{B}}T}\right)$$

where c_{ref} is the monomer concentration under the reference pressure of 1 atm, and ΔG_i is the Gibbs free energy of the formation of cluster i.

The formation of clusters is accompanied by the competition between collision and evaporation. The clusters with a collision frequency higher than the total evaporation frequency ($\beta c/\Sigma\gamma$>1) are considered to be stable in the perspective of nucleation kinetics. The detailed collision and total evaporation frequencies of the HIO_3-HIO_2-DMA system at all simulated temperatures and condensation sinks are listed in Tables S1-S4. The boundary conditions of the ACDC simulations are closely related to the ratio of the collision frequency between the clusters and monomer molecule at the concentration c to the total evaporation frequency of clusters (details in Section S1).

https://doi.org/10.5194/egusphere-2023-1774
Preprint. Discussion started: 17 October 2023

3 Results

3.1 Cluster stable configurations

In order to evaluate the interacting potential of HIO_3, HIO_2, and DMA, the electrostatic potential (ESP) distribution on the molecular van der Waal (vdW) surfaces of three monomer molecules was determined by the Visual Molecular Dynamics (VMD) (Humphrey et al., 1996) and the Multiwfn 3.7 program. In general, the sites with maximum ESP values, which possess electron-deficient properties, on the molecular surface tend to attract the electron-rich regions with minimum ESP values to form non-covalent interactions, such as hydrogen bonds (HBs) or halogen bonds (XBs). Fig. 1 illustrates the presence of interaction regions on the surfaces of HIO_3, HIO_2, and DMA, characterized by positive or negative ESP values. DMA has a -NH group which can act as both donor and acceptor of non-covalent interactions, so that DMA can potentially form a spatial network structure with iodine oxoacids through HBs or XBs, providing possibility to form stable clusters.

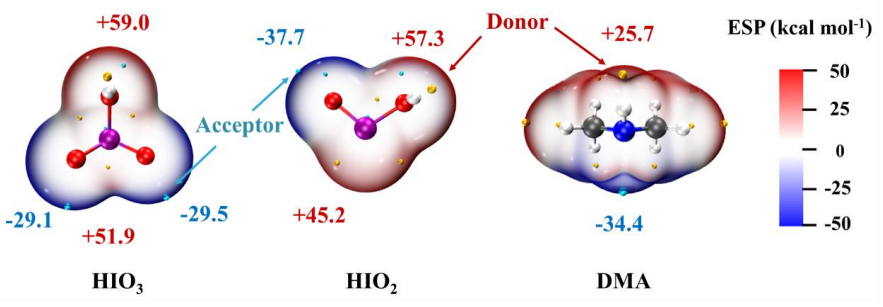

Figure 1. The ESP-mapped molecular van der Waals (vdW) surfaces of the HIO_3, HIO_2, and DMA monomer at the ωB97X-D/6-311++G(3df,3pd) (for H, C, N and O atoms) + aug-cc-pVTZ-PP with ECP28MDF (for I atom) level of theory. The yellow and cyan dots represent the maximum and minimum points of the ESP, respectively. The white, grey, blue, red, and purple spheres represent the H, C, N, O, and I atoms, respectively. The unit of ESP is kcal mol^{-1}.

The most stable configurations of the HIO_3-HIO_2-DMA ternary clusters at the ωB97X-D/6-311++G(3df,3pd) (for H, C, N, and O atoms) + aug-cc-pVTZ-PP with ECP28MDF (for I atom) level of theory are shown in Fig. 2. The structures of the HIO_2-DMA clusters can be found in Fig. S1 of the Supplementary Information, and the cartesian coordinates of all HIO_3-HIO_2-DMA and HIO_2-DMA clusters are shown in Table S5. As can be seen from Fig. 2, DMA can form stable ternary clusters through the space network formed by HBs and XBs, which proves the prediction of electrostatic potential analysis. Moreover, acid-base proton transfer can be found in all ternary clusters except for the $(HIO_3)_1(HIO_2)_2(DMA)_1$ cluster. It has been shown in the previous study on HIO_3-DMA and HIO_3-HIO_2 systems that acid-base proton transfer occurred between HIO_3 and HIO_2/DMA (Zhang et al., 2022a; Ning et al., 2022; Liu et al., 2023). DMA is capable to efficiently stabilize acidic precursors, and HIO_2 can also act as a stabilizing base in the neutral nucleation process of HIO_3-HIO_2 (Zhang et al., 2022a; Liu et al., 2023). Hence, the participation of DMA may potentially lead to a competition between two basic molecules for proton transfer reaction.

https://doi.org/10.5194/egusphere-2023-1774
Preprint. Discussion started: 17 October 2023

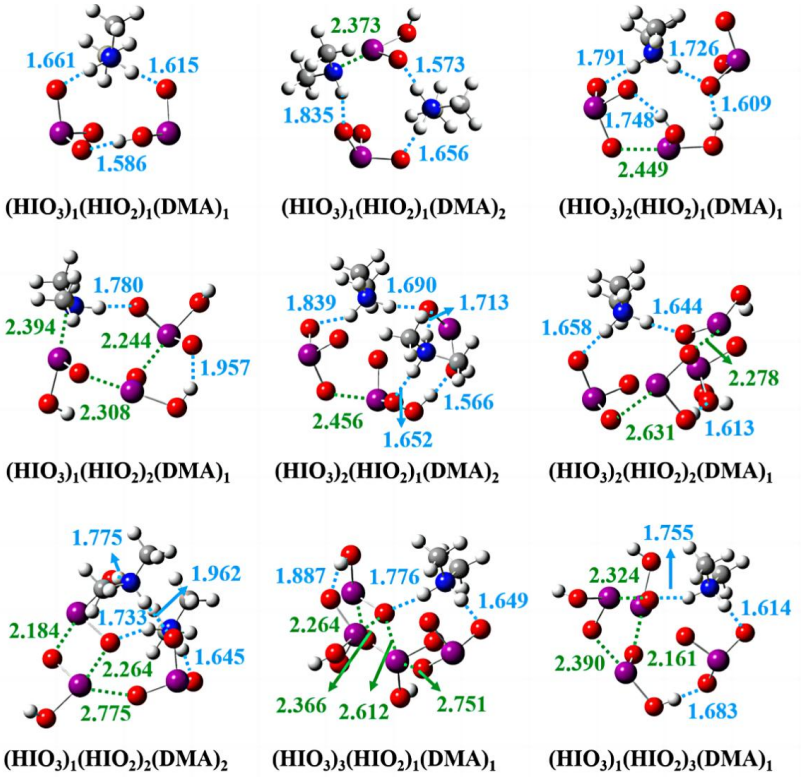

Figure 2. The most stable structures of HIO_3-HIO_2-DMA clusters identified at the ωB97X-D/6-311++G(3df,3pd) (for H, C, N and O atoms) + aug-cc-pVTZ-PP with ECP28MDF (for I atom) level of theory. The white, grey, blue, red, and purple balls represent the H, C, N, O and I atoms, respectively. The hydrogen bonds and halogen bonds are shown in blue and green dashed lines, respectively. The values of bond lengths are given in Å.

In order to assess the effect of DMA on the proton transfer process, the analysis of the proton transfer was performed based on the change of bond length at corresponding positions that conduct acid-base reaction. The number of proton transfer between different precursors in ternary clusters and the total number of proton transfer are summarized in Table S6. As shown in Table S6, among most of the ternary clusters, HIO_3 will preferentially interact with DMA, which possesses relatively stronger basicity than HIO_2 in the process of proton transfer. Afterwards, the remaining HIO_3 can perform proton transfer with the amphoteric HIO_2, which acts as a relatively week base under the circumstance. In summary, the structural analysis shows that DMA can form stable clusters with iodine oxoacids via HBs, XBs and proton transfer, laying the foundation for promoting HIO_3-HIO_2 nucleation. Moreover, DMA competes with HIO_2 to accept the proton from HIO_3 in the most stable configurations of HIO_3-HIO_2-DMA clusters, which indicates a potential competition between two basic molecules in the following nucleation process.

3.2 Cluster formation pathways

To further study the kinetic behavior of DMA in nucleation process, the ACDC was used to simulate the nucleation pathways under marine atmospheric conditions. Firstly, a specific simulation was performed under atmospheric conditions reported in the field observation of Mace Head (Sipila et al., 2016), a research station at the west coast of Ireland. The main cluster formation pathways, which contributes more than 5% to the total cluster formation rates, at [HIO_3] of 1.0×10^8 molecules cm^{-3}, [HIO_2] of 2.0×10^6 molecules cm^{-3} and 287 K are shown in Fig. 3. Field observations of [DMA] in Mace Head are lacking. Hence, according to the results of GEOS-Chem model simulation (Yu and Luo, 2014), we chose the lowest

https://doi.org/10.5194/egusphere-2023-1774
Preprint. Discussion started: 17 October 2023

[DMA] of 5.0 × 10^5 molecules cm^{-3}. The average condensation sink (CS) was estimated and set to be 2.0 × 10^{-3} s^{-1} for coastal regions (Dal Maso et al., 2002). As shown in Fig. 3, DMA can be significantly involved in the nucleation process of the HIO_3-HIO_2 system at the lowest DMA concentration. The pathway of HIO_3-HIO_2-DMA ternary nucleation contributes 38% to the total nucleation pathways, indicating an important contribution of HIO_3-HIO_2 nucleation with the involvement of DMA to the marine NPF events. The detailed description of nucleation pathway can be seen from Supplementary Information (Section S2). The field observations (Sipila et al., 2016) did not mention the DMA-containing clusters in the nucleation of HIO_3, which was speculated to be concerned with the low probability of detection due to both of the low concentration of DMA and the evaporation of DMA after DMA-containing clusters entering the mass spectrum with ionization (Kurten et al., 2011).

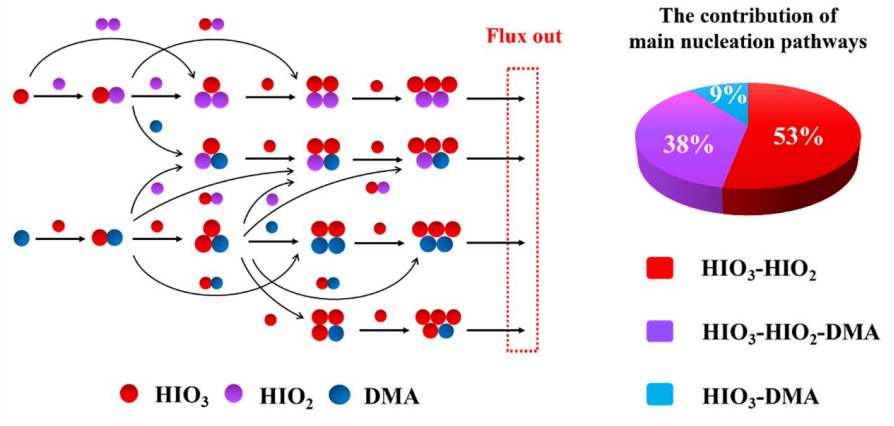

Figure 3. The cluster formation pathways and the contribution of main pathways to the total cluster formation rates under field conditions of Mace Head at [HIO_3] of 1.0 × 10^8 molecules cm^{-3}, [HIO_2] of 2.0 × 10^6 molecules cm^{-3}, [DMA] of 5.0 × 10^5 molecules cm^{-3}, T = 287 K, and CS = 2.0 × 10^{-3} s^{-1}. The red, purple, and blue balls represent the HIO_3, HIO_2, and DMA molecules, respectively. The proportion of the contribution of HIO_3-HIO_2, HIO_3-HIO_2-DMA, and HIO_3-DMA are shown in red, purple, and blue, respectively.

The simulated nucleation pathway under the specific condition has proved the participation of DMA in HIO_3-HIO_2 nucleation. However, since HIO_x (x = 2, 3) and DMA originate from different sources, the concentrations of precursors should be changed to better represent the situation of regions with different iodine and amine emission intensities. Therefore, to further study the involvement of DMA in nucleation pathways under various oceanic atmospheric conditions, the contribution of the main cluster formation pathways at different concentrations are simulated and the results are shown in Fig. 4. It is worth noting that the concentration of HIO_2 changes together with that of HIO_3 from low to high since HIO_2 and HIO_3 are homologous iodine species. The ratio of [HIO_3] to [HIO_2] is about 20 to 100 depending on the concentration of iodine vapor (Sipila et al., 2016; He et al., 2021). The ratio used in Fig. 4 was 50 according to the former field observations in Mace Head (Sipila et al., 2016) and the other results obtained from two different ratios (20 and 100) of [HIO_3] and [HIO_2] can be seen from the Section S3 of the Supplementary Information.

As can be seen from Fig. 4, the contribution of DMA to the nucleation increases with [DMA] rising from 10^4 to 10^8 molecules cm^{-3}, and the dominating mechanism varies from HIO_3-HIO_2 nucleation to HIO_3-HIO_2-DMA nucleation and then to HIO_3-DMA nucleation. The proportion of HIO_3-HIO_2 binary pathway rises together with the increase of [HIO_x] (x = 2, 3). The involvement of DMA in the pathways of HIO_3-HIO_2 nucleation is significant and the ternary nucleation pathway is more important than HIO_3-HIO_2 nucleation pathway when [DMA] is half the concentration of [HIO_2] (indicated by the red dashed line in Fig. 4). The HIO_3-HIO_2-DMA mechanism strives essentially from the competitiveness of the two base molecules, DMA and HIO_2, and the HIO_3-HIO_2-DMA ternary nucleation is critical in explaining the missing sources of new particles especially in the place where the concentrations of HIO_2 and DMA are similar. In contrast, when one base is much more

https://doi.org/10.5194/egusphere-2023-1774
Preprint. Discussion started: 17 October 2023

abundant than the other, the pathways are overwhelmingly dominated by rapid binary nucleation involving HIO_3 and the base with higher concentration. This is the first time that a combined influence of multiple bases has been discovered in the nucleation process driven by HIO_3, which manifests as competition in the nucleation pathways varied with concentrations.

Overall, the simulated contributions of different nucleation pathways under a wide range of the concentrations of precursors have indicated a significant participation of DMA in HIO_3-HIO_2 nucleation. Notably, both DMA and HIO_2 act as stabilizing bases, and the competition between DMA and HIO_2 determines their contributions to the nucleation pathways. The ternary mechanism dominates the nucleation process especially in the regions with similar [HIO_2] and [DMA] concentrations (up to 69%). When [DMA] is at least one order of magnitude higher than [HIO_2], the HIO_3-DMA binary nucleation mechanism will turn to be the dominated pathways. These results may explain some of the missing sources in marine NPF and help to better understand the competition of bases (HIO_2 and DMA) in HIO_3 nucleation.

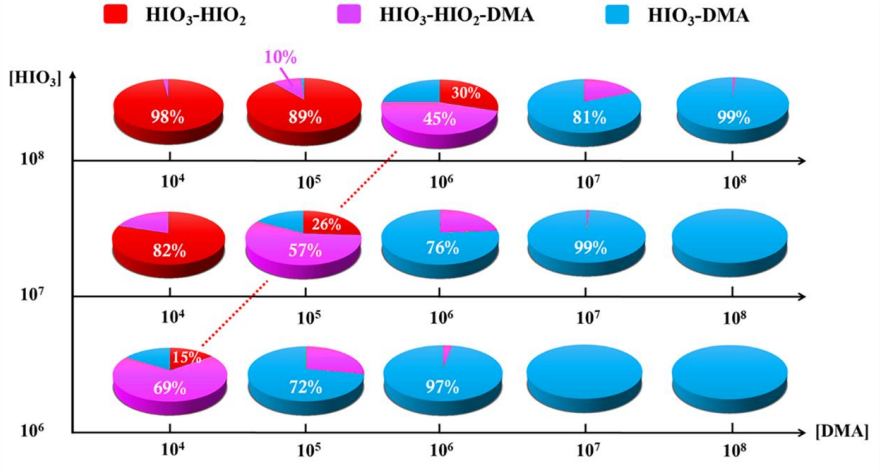

Figure 4. The contribution of main nucleation pathways at different concentrations of precursors. [HIO_3] = 10^6 − 10^8 molecules cm^{-3}, [HIO_2] = 2.0×10^4 − 2.0×10^6 molecules cm^{-3} and [DMA] = 10^4 − 10^8 molecules cm^{-3}. The simulated temperature and condensation sink are 283 K and 2.0×10^{-3} s^{-1} as typical values for oceanic atmosphere. The proportion of the contribution of HIO_3-HIO_2, HIO_3-HIO_2-DMA, and HIO_3-DMA are shown in red, purple, and blue, respectively. The pie chart connected by red dashed line indicates the significant contribution of ternary nucleation to the nucleation pathways.

3.3 Cluster formation rates

The cluster formation pathway showed that DMA can significantly participate in the HIO_3-HIO_2 nucleation. However, the influence of DMA on the cluster formation rates (J) of the HIO_3-HIO_2 nucleation is still unknown. Iodine oxoacids have been reported to cause NPF events in mid-latitude coastal and high-latitude polar regions (Sipila et al., 2016; Yu et al., 2019; Baccarini et al., 2020; Rong et al., 2020; Xia et al., 2020; He et al., 2021). Therefore, the cluster formation rates of HIO_3-HIO_2-DMA nucleation and HIO_3-HIO_2 nucleation were simulated under three different conditions corresponding to three typical field situations (the west coast of Ireland, the southeast coast of China, and the Aboa station in Antarctic) in order to further evaluate the actual effect of DMA on the J of HIO_3-HIO_2 nucleation.

Mace Head, the west coast of Ireland, has strong iodine emissions, but the sources of amine are relatively insufficient, which may lead to a low concentration of DMA in the gas phase. The J of HIO_3-HIO_2-DMA and HIO_3-HIO_2 in Mace Head are shown in Fig. 5 (a) at T = 287 K, CS = 2.0×10^{-3} s^{-1}, [HIO_3] = 10^7 − 10^8 molecules cm^{-3}, and [HIO_2] = 2.0×10^5 − 2.0×10^6 molecules cm^{-3} (Sipila et al., 2016; He et al., 2021). The simulated J of HIO_3-HIO_2-DMA and HIO_3-HIO_2 are rising along with the increase of [HIO_3] and [HIO_2], and the involvement of DMA on a scale of 5.0×10^5 to 5.0×10^7 molecules

https://doi.org/10.5194/egusphere-2023-1774
Preprint. Discussion started: 17 October 2023

cm^{-3} acquired from model simulation (Yu and Luo, 2014) can enhance the *J*. The *J* of HIO_3-HIO_2 binary nucleation can reach the reported field observation value (Sipila et al., 2016) of 10^4 cm^{-3} s^{-1} at high concentrations of precursors, emphasizing the importance of iodine oxoacids nucleation. The *J* enhanced by DMA can match higher values ranging from 10^4 to 10^6 cm^{-3} s^{-1} reported by the field observations (O'dowd et al., 2002b), and the same *J* can be acquired at a lower concentration of the iodine oxoacids (Fig. S5) with the participation of DMA. To assess the enhancement effects of DMA, the enhancement factor (*R*) is defined as the ratio of the *J* of HIO_3-HIO_2-DMA to the *J* of HIO_3-HIO_2. The *R* is plotted against the concentrations of the precursors in Fig. 5 (b). As can be seen, *R* increases from 10^0 to 10^4 with the increase of [DMA] as well as the decrease of [HIO_3] and [HIO_2]. Even at high [HIO_x] (x = 2, 3) and low [DMA], DMA can also slightly enhance the cluster formation rates by 1.5 – 10 times, which is attributed to the strong nucleation ability of DMA. Therefore, the role of DMA should not be ignored in those regions with abundant iodine and scarce amine concentrations similar to Mace Head especially when there are intensive NPF events with high *J*.

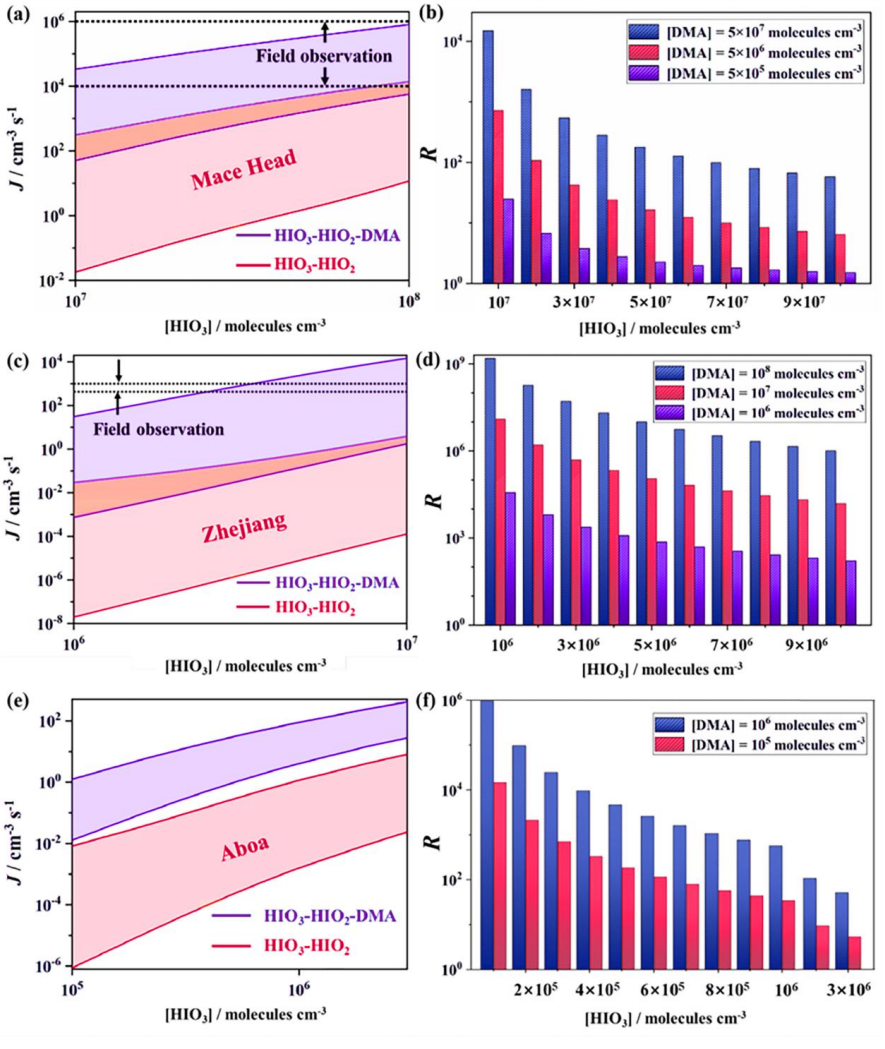

Figure 5. The cluster formation rates (*J*, cm^{-3} s^{-1}) and the enhancement factor (*R*) at varying atmospheric conditions of **(a)** and **(b)** Mace Head, the west coast of Ireland ([DMA] = 5.0 × 10^5 − 5.0 × 10^7 molecules cm^{-3}), **(c)** and **(d)** Zhejiang, the southeast coast of China ([DMA] = 10^6 − 10^8 molecules cm^{-3}), **(e)** and **(f)** Aboa station in Antarctic ([DMA] = 10^6 – 10^7

https://doi.org/10.5194/egusphere-2023-1774
Preprint. Discussion started: 17 October 2023

molecules cm^{-3}). The black dashed line indicates the J in field observation.

Zhejiang, the southeast coast of China, has been proved to be one of the strongest sources of gaseous DMA in marine areas (Muller et al., 2009; Hu et al., 2015; Chen et al., 2021). Zhejiang represents those regions with relatively high [DMA] and relatively low [HIO_x] (x = 2, 3). The J of HIO_3-HIO_2-DMA and HIO_3-HIO_2 in Zhejiang are shown in Fig. 5 (c) at T = 290 K, CS = 1×10^{-2} s^{-1}, [HIO_3] = $10^6 - 10^7$ molecules cm^{-3}, [HIO_2] = $2.0 \times 10^4 - 2.0 \times 10^5$ molecules cm^{-3}, and [DMA] = $10^6 - 10^8$ molecules cm^{-3} (Sipila et al., 2016; Yu et al., 2019; He et al., 2021; Chen et al., 2022). As shown in Fig. 5 (c), the J changes in direct proportion to [HIO_3] and [DMA]. The J of HIO_3-HIO_2 is lower than reported rates ranging from 4.2×10^2 to 1.0×10^3 cm^{-3} s^{-1} in Zhejiang (Yu et al., 2019; Xia et al., 2020). As shown in Fig. 5(d), R varies from 10^3 to 10^9 with the increase of [DMA], which indicates that the J is sensitive to the concentration of DMA. The participation of DMA with high concentrations of $10^7 - 10^8$ molecules cm^{-3} can bridge the gap between HIO_3-HIO_2 nucleation mechanism and the field observations with an enhancement over 10^3-fold to J. Thus, DMA plays a critical role in enhancing the J in areas with strong amine emissions and relatively insufficient iodine sources.

The Aboa station in Antarctic represents the ice-covered polar regions with low level of iodine and amine emissions. The J and R of HIO_3-HIO_2-DMA and HIO_3-HIO_2 under polar conditions are shown in Figs. 5 (e) and (f) at T = 268 K, CS = 1.0×10^{-4} s^{-1}, [HIO_3] = $10^5 - 3.0 \times 10^6$ molecules cm^{-3}, [HIO_2] = $2.0 \times 10^3 - 6.0 \times 10^4$ molecules cm^{-3}, and [DMA] = $10^5 - 10^6$ molecules cm^{-3} (Yu and Luo, 2014; Sipila et al., 2016; He et al., 2021). As can be seen from Figs. 5 (e) and (f), the generally low concentrations of iodine oxoacids in the polar regions may lead to the less importance of iodine nucleation, but the J of HIO_3-HIO_2-DMA is at least two orders of magnitude higher than HIO_3-HIO_2 nucleation even at the low level of [DMA]. In polar regions with poor emissions of precursors, the enhancement of DMA is still significant, and HIO_3-HIO_2-DMA ternary nucleation will become a more potential mechanism than HIO_3-HIO_2, which deserves more attention in the future to verify the importance.

Overall, the J of HIO_3-HIO_2-DMA nucleation is higher than that of HIO_3-HIO_2 in broad marine areas, which can shed light on the vital enhancement of DMA on HIO_3-HIO_2 nucleation. Especially, DMA can significantly enhance the J of HIO_3-HIO_2 by more than 10^3-fold in regions with abundant amine and scarce iodine. These results can to some extent fill in the gaps between the J of HIO_3-HIO_2 nucleation and the field observations.

4 Atmospheric significance and conclusion

The present study investigated the iodine oxoacids nucleation enhanced by DMA under broad oceanic atmospheric conditions by the quantum chemical calculations combined with ACDC simulations. As a basic precursor to stabilize acid, DMA can form the stable ternary clusters with HIO_3 and HIO_2, in which DMA can compete with HIO_2 to accept the proton from HIO_3. Kinetically, DMA can participate in the HIO_3-HIO_2 nucleation pathways, and the contribution of HIO_3-HIO_2-DMA to the nucleation pathways can be up to 69%. Moreover, the simulated J shows that in marine regions with abundant iodine and scarce amine concentrations, such as Mace Head, DMA can slightly enhance the J by 1.5 – 10 times, appropriately matching the J in local measurement of intensive NPF events. In marine regions with scarce iodine and abundant amine concentrations, such as Zhejiang, DMA can bridge the gap between HIO_3-HIO_2 nucleation mechanism and the field observations through a significant enhancement by more than 10^3-fold to J. And in ice-covered polar regions with low level of iodine and amine emissions, such as the Aboa station, the J of HIO_3-HIO_2-DMA is at least two orders of magnitude higher than HIO_3-HIO_2 nucleation, indicating that the enhancement of DMA is still significant in polar regions with low [DMA]. Therefore, DMA significantly enhances the J of HIO_3-HIO_2 nucleation in broad marine regions, especially in marine regions with abundant amine and scarce iodine and establishes reasonable connections between the widely concerned iodine oxoacids nucleation and the rapid formation of marine new particles by enhancing J. However, considering the conditions of humidity in oceanic atmosphere and the complexity of marine NPF events, future research should investigate the role of water molecules and other crucial precursors to establish a comprehensive multi-component nucleation mechanism in the marine atmosphere.

https://doi.org/10.5194/egusphere-2023-1774
Preprint. Discussion started: 17 October 2023

Data availability

The data in this article can be available from the corresponding author upon request (lingliu@bit.edu.cn and zhangxiuhui@bit.edu.cn).

Supplement

The supplement related to this article is available online at: XXXXXXXX.

Author contributions

XZ designed and supervised the research. HZ performed the quantum chemical calculations and the ACDC simulations. HZ and LL analyzed data. HZ, LL and XZ wrote the paper. XZ, LL, BC, and YL reviewed and edited the paper. All authors commented on the paper.

Competing interests

The contact author has declared that neither they nor their co-authors have any competing interests.

Disclaimer

Publisher's note: Copernicus Publications remains neutral with regard to jurisdictional claims in published maps and institutional affiliations.

Acknowledgements

We acknowledge the National Supercomputing Center in Shenzhen for providing the computational resources and the Turbomole program.

Financial support

This work is supported by the National Science Fund for Distinguished Young Scholars (grant no. 22225607) and the National Natural Science Foundation of China (grant nos. 21976015, 42105101, and 22122610).

References

Ahlrichs, R., Bar, M., Haser, M., Horn, H., and Kolmel, C.: Electronic-structure calculations on workstation computers - the program system turbomole, Chem. Phys. Lett., 162, 165-169, https://doi.org/10.1016/0009-2614(89)85118-8, 1989.

Almeida, J., Schobesberger, S., Kurten, A., Ortega, I. K., Kupiainen-Maatta, O., Praplan, A. P., Adamov, A., Amorim, A., Bianchi, F., Breitenlechner, M., David, A., Dommen, J., Donahue, N. M., Downard, A., Dunne, E., Duplissy, J., Ehrhart, S., Flagan, R. C., Franchin, A., Guida, R., Hakala, J., Hansel, A., Heinritzi, M., Henschel, H., Jokinen, T., Junninen, H., Kajos, M., Kangasluoma, J., Keskinen, H., Kupc, A., Kurten, T., Kvashin, A. N., Laaksonen, A., Lehtipalo, K., Leiminger, M., Leppa, J., Loukonen, V., Makhmutov, V., Mathot, S., McGrath, M. J., Nieminen, T., Olenius, T., Onnela, A., Petaja, T., Riccobono, F., Riipinen, I., Rissanen, M., Rondo, L., Ruuskanen, T., Santos, F. D., Sarnela, N., Schallhart, S., Schnitzhofer, R., Seinfeld, J. H., Simon, M., Sipila, M., Stozhkov, Y., Stratmann, F., Tome, A., Trostl, J., Tsagkogeorgas, G., Vaattovaara, P., Viisanen, Y., Virtanen, A., Vrtala, A., Wagner, P. E., Weingartner, E., Wex, H., Williamson, C., Wimmer, D., Ye, P. L., Yli-Juuti, T., Carslaw, K. S., Kulmala, M., Curtius, J., Baltensperger, U., Worsnop, D. R., Vehkamaki, H., and Kirkby, J.: Molecular understanding of sulphuric acid-amine particle nucleation in the atmosphere, Nature, 502, 359-363, https://doi.org/10.1038/nature12663, 2013.

Baccarini, A., Karlsson, L., Dommen, J., Duplessis, P., Vullers, J., Brooks, I. M., Saiz-Lopez, A., Salter, M., Tjernstrom, M., Baltensperger, U., Zieger, P., and Schmale, J.: Frequent new particle formation over the high Arctic pack ice by enhanced iodine emissions, Nat. Commun., 11, https://doi.org/10.1038/s41467-020-18551-0, 2020.

Chai, J. D. and Head-Gordon, M.: Long-range corrected hybrid density functionals with damped atom-atom dispersion corrections, Phys. Chem. Chem. Phys., 10, 6615-6620, https://doi.org/10.1039/b810189b, 2008.

https://doi.org/10.5194/egusphere-2023-1774
Preprint. Discussion started: 17 October 2023

Chen, D. H., Shen, Y. J., Wang, J. T., Gao, Y., Gao, H. W., and Yao, X. H.: Mapping gaseous dimethylamine, trimethylamine, ammonia, and their particulate counterparts in marine atmospheres of China's marginal seas - Part 1: Differentiating marine emission from continental transport, Atmos. Chem. Phys., 21, 16413-16425, https://doi.org/10.5194/acp-21-16413-2021, 2021.

Chen, D. H., Yao, X. H., Chan, C. K., Tian, X. M., Chu, Y. X., Clegg, S. L., Shen, Y. J., Gao, Y., and Gao, H. W.: Competitive uptake of dimethylamine and trimethylamine against ammonia on acidic particles in marine atmospheres, Environ. Sci. Technol., 56, 5430-5439, https://doi.org/10.1021/acs.est.1c08713, 2022.

Dal Maso, M., Kulmala, M., Lehtinen, K., Makela, J., Aalto, P., and O'Dowd, C.: Condensation and coagulation sinks and formation of nucleation mode particles in coastal and boreal forest boundary layers, J. Geophys. Res.: Atmos., 107, 8097, https://doi.org/10.1029/2001jd001053, 2002.

Dall'Osto, M., Airs, R. L., Beale, R., Cree, C., Fitzsimons, M. F., Beddows, D., Harrison, R. M., Ceburnis, D., O'Dowd, C., Rinaldi, M., Paglione, M., Nenes, A., Decesari, S., and Simo, R.: Simultaneous detection of alkylamines in the surface ocean and atmosphere of the antarctic sympagic environment, ACS Earth Space Chem., 3, 854-862, https://doi.org/10.1021/acsearthspacechem.9b00028, 2019.

Dall'Osto, M., Beddows, D. C. S., Tunved, P., Krejci, R., Strom, J., Hansson, H. C., Yoon, Y. J., Park, K. T., Becagli, S., Udisti, R., Onasch, T., O'Dowd, C. D., Simo, R., and Harrison, R. M.: Arctic sea ice melt leads to atmospheric new particle formation, Sci. Rep., 7, https://doi.org/10.1038/s41598-017-03328-1, 2017.

Ehn, M., Vuollekoski, H., Petaja, T., Kerminen, V. M., Vana, M., Aalto, P., de Leeuw, G., Ceburnis, D., Dupuy, R., O'Dowd, C. D., and Kulmala, M.: Growth rates during coastal and marine new particle formation in western Ireland, J. Geophys. Res.: Atmos., 115, https://doi.org/10.1029/2010jd014292, 2010.

Elm, J. and Kristensen, K.: Basis set convergence of the binding energies of strongly hydrogen-bonded atmospheric clusters, Phys. Chem. Chem. Phys., 19, 1122-1133, https://doi.org/10.1039/c6cp06851k, 2017.

Elm, J., Bilde, M., and Mikkelsen, K. V.: Assessment of binding energies of atmospherically relevant clusters, Phys. Chem. Chem. Phys., 15, 16442-16445, https://doi.org/10.1039/c3cp52616j, 2013.

Facchini, M. C., Decesari, S., Rinaldi, M., Carbone, C., Finessi, E., Mircea, M., Fuzzi, S., Moretti, F., Tagliavini, E., Ceburnis, D., and O'Dowd, C. D.: Important source of marine secondary organic aerosol from biogenic amines, Environ. Sci. Technol., 42, 9116-9121, https://doi.org/10.1021/es8018385, 2008.

Frisch, M. J., Pople, J. A., and Binkley, J. S.: Self-consistent molecular orbital methods 25. Supplementary functions for Gaussian basis sets, J. Chem. Phys., 80, 3265-3269, https://doi.org/10.1063/1.447079, 1984.

Frisch, M. J., Trucks, G.W., Schlegel, H.B., Scuseria, G.E., Robb, M.A., Cheeseman, J.R.,, Scalmani, G., Barone, V., Mennucci, B., Petersson, G.A., Nakatsuji, H., Caricato, M.,, Li, X., Hratchian, H.P., Izmaylov, A.F., Bloino, J., Zheng, G., Sonnenberg, J.L., Hada,, M., E., M., Toyota, K., Fukuda, R., Hasegawa, J., Ishida, M., Nakajima, T., Honda,, Y., K., O., Nakai, H., Vreven, T., Montgomery, J.A., Peralta, J.E., Ogliaro, F.,, Bearpark, M., Heyd, J.J., Brothers, E., Kudin, K.N., Staroverov, V.N., Kobayashi, R.,, Normand, J., Raghavachari, K., Rendell, A., Burant, J.C., Iyengar, S.S., Tomasi, J.,, Cossi, M., Rega, N., Millam, J.M., Klene, M., Knox, J.E., Cross, J.B., Bakken, V.,, Adamo, C., Jaramillo, J., Gomperts, R., Stratmann, R.E., Yazyev, O., Austin, A.J.,, Cammi, R., Pomelli, C., Ochterski, J.W., Martin, R.L., Morokuma, K., Zakrzewski,, V.G., V., G.A., Salvador, P., Dannenberg, J.J., Dapprich, S., Daniels, A.D., Farkas,, and O., F., J.B., Ortiz, J.V., Cioslowski, J., Fox, D.J.: Gaussian 09, Revision A.1. Gaussian Inc, Wallingford CT., Gaussian 09, Revision A.1. Gaussian Inc, Wallingford CT., 2009.

Gibb, S. W., Mantoura, R. F. C., and Liss, P. S.: Ocean-atmosphere exchange and atmospheric speciation of ammonia and methylamines in the region of the NW Arabian Sea, Global Biogeochem. Cycles, 13, 161-177, https://doi.org/10.1029/98gb00743, 1999.

Gong, J., Zhu, T., Kipen, H., Wang, G., Hu, M., Guo, Q., Ohman-Strickland, P., Lu, S. E., Wang, Y., Zhu, P., Rich, D. Q., Huang, W., and Zhang, J.: Comparisons of ultrafine and fine particles in their associations with biomarkers reflecting physiological pathways, Environ. Sci. Technol., 48, 5264-5273, https://doi.org/10.1021/es5006016, 2014.

Gronberg, L., Lovkvist, P., and Jonsson, J. A.: Measurement of aliphatic amines in ambient air and rainwater, Chemosphere, 24, 1533-1540, https://doi.org/10.1016/0045-6535(92)90273-t, 1992.

https://doi.org/10.5194/egusphere-2023-1774
Preprint. Discussion started: 17 October 2023

Haywood, J. and Boucher, O.: Estimates of the direct and indirect radiative forcing due to tropospheric aerosols: A review, Rev. Geophys., 38, 513-543, https://doi.org/10.1029/1999rg000078, 2000.

He, X. C., Tham, Y. J., Dada, L., Wang, M. Y., Finkenzeller, H., Stolzenburg, D., Iyer, S., Simon, M., Kurten, A., Shen, J. L., Rorup, B., Rissanen, M., Schobesberger, S., Baalbaki, R., Wang, D. S., Koenig, T. K., Jokinen, T., Sarnela, N., Beck, L. J., Almeida, J., Amanatidis, S., Amorim, A., Ataei, F., Baccarini, A., Bertozzi, B., Bianchi, F., Brilke, S., Caudillo, L., Chen, D. X., Chiu, R., Chu, B. W., Dias, A., Ding, A. J., Dommen, J., Duplissy, J., El Haddad, I., Carracedo, L. G., Granzin, M., Hansel, A., Heinritzi, M., Hofbauer, V., Junninen, H., Kangasluoma, J., Kemppainen, D., Kim, C., Kong, W. M., Krechmer, J. E., Kvashin, A., Laitinen, T., Lamkaddam, H., Lee, C. P., Lehtipalo, K., Leiminger, M., Li, Z. J., Makhmutov, V., Manninen, H. E., Marie, G., Marten, R., Mathot, S., Mauldin, R. L., Mentler, B., Mohler, O., Muller, T., Nie, W., Onnela, A., Petaja, T., Pfeifer, J., Philippov, M., Ranjithkumar, A., Saiz-Lopez, A., Salma, I., Scholz, W., Schuchmann, S., Schulze, B., Steiner, G., Stozhkov, Y., Tauber, C., Tome, A., Thakur, R. C., Vaisanen, O., Vazquez-Pufleau, M., Wagner, A. C., Wang, Y. H., Weber, S. K., Winkler, P. M., Wu, Y. S., Xiao, M., Yan, C., Ye, Q., Ylisirnio, A., Zauner-Wieczorek, M., Zha, Q. Z., Zhou, P. T., Flagan, R. C., Curtius, J., Baltensperger, U., Kulmala, M., Kerminen, V. M., Kurten, T., Donahue, N. M., Volkamer, R., Kirkby, J., Worsnop, D. R., and Sipila, M.: Role of iodine oxoacids in atmospheric aerosol nucleation, Science, 371, 589-595, https://doi.org/10.1126/science.abe0298, 2021.

Hoffmann, T., O'Dowd, C. D., and Seinfeld, J. H.: Iodine oxide homogeneous nucleation: An explanation for coastal new particle production, Geophys. Res. Lett., 28, 1949-1952, https://doi.org/10.1029/2000gl012399, 2001.

Hu, Q. J., Yu, P. R., Zhu, Y. J., Li, K., Gao, H. W., and Yao, X. H.: Concentration, size distribution, and formation of trimethylaminium and dimethylaminium ions in atmospheric particles over marginal seas of China, J. Atmos. Sci., 72, 3487-3498, https://doi.org/10.1175/jas-d-14-0393.1, 2015.

Humphrey, W., Dalke, A., and Schulten, K.: VMD: Visual molecular dynamics, J. Mol. Graphics Modell., 14, 33-38, https://doi.org/10.1016/0263-7855(96)00018-5, 1996.

Kalivitis, N., Kerminen, V. M., Kouvarakis, G., Stavroulas, I., Bougiatioti, A., Nenes, A., Manninen, H. E., Petaja, T., Kulmala, M., and Mihalopoulos, N.: Atmospheric new particle formation as a source of CCN in the eastern Mediterranean marine boundary layer, Atmos. Chem. Phys., 15, 9203-9215, https://doi.org/10.5194/acp-15-9203-2015, 2015.

Kuerten, A., Li, C., Bianchi, F., Curtius, J., Dias, A., Donahue, N. M., Duplissy, J., Flagan, R. C., Hakala, J., Jokinen, T., Kirkby, J., Kulmala, M., Laaksonen, A., Lehtipalo, K., Makhmutov, V., Onnela, A., Rissanen, M. P., Simon, M., Sipila, M., Stozhkov, Y., Trostl, J., Ye, P., and McMurry, P. H.: New particle formation in the sulfuric acid-dimethylamine-water system: reevaluation of CLOUD chamber measurements and comparison to an aerosol nucleation and growth model, Atmos. Chem. Phys., 18, 845-863, https://doi.org/10.5194/acp-18-845-2018, 2018.

Kurten, T., Petaja, T., Smith, J., Ortega, I. K., Sipila, M., Junninen, H., Ehn, M., Vehkamaki, H., Mauldin, L., Worsnop, D. R., and Kulmala, M.: The effect of H2SO4 - amine clustering on chemical ionization mass spectrometry (CIMS) measurements of gas-phase sulfuric acid, Atmos. Chem. Phys., 11, 3007-3019, https://doi.org/10.5194/acp-11-3007-2011, 2011.

Lee, S. H., Gordon, H., Yu, H., Lehtipalo, K., Haley, R., Li, Y. X., and Zhang, R. Y.: New particle formation in the atmosphere: From molecular clusters to global climate, J. Geophys. Res.: Atmos., 124, 7098-7146, https://doi.org/10.1029/2018jd029356, 2019.

Liu, L., Li, S. N., Zu, H. T., and Zhang, X. H.: Unexpectedly significant stabilizing mechanism of iodous acid on iodic acid nucleation under different atmospheric conditions, Sci. Total Environ., 859, 159832, https://doi.org/10.1016/j.scitotenv.2022.159832, 2023.

Lu, T. and Chen, F.: Quantitative analysis of molecular surface based on improved Marching Tetrahedra algorithm, J. Mol. Graphics Modell., 38, 314-323, https://doi.org/10.1016/j.jmgm.2012.07.004, 2012a.

Lu, T. and Chen, F. W.: Multiwfn: A multifunctional wavefunction analyzer, J. Comput. Chem., 33, 580-592, https://doi.org/10.1002/jcc.22885, 2012b.

Lu, Y. Q., Liu, L., Ning, A., Yang, G., Liu, Y. L., Kurten, T., Vehkamaki, H., Zhang, X. H., and Wang, L.: Atmospheric sulfuric acid-dimethylamine nucleation enhanced by trifluoroacetic acid, Geophys. Res. Lett., 47, https://doi.org/10.1029/2019gl085627, 2020.

Ma, F. F., Xie, H. B., Zhang, R. J., Su, L. H., Jiang, Q., Tang, W. H., Chen, J. W., Engsvang, M., Elm, J., and He, X. C.:

https://doi.org/10.5194/egusphere-2023-1774
Preprint. Discussion started: 17 October 2023

Enhancement of atmospheric nucleation precursors on iodic acid-induced nucleation: Predictive model and mechanism, Environ. Sci. Technol., 57, 6944-6954, https://doi.org/10.1021/acs.est.3c01034, 2023.

Mahajan, A. S., Sorribas, M., Martin, J. C. G., MacDonald, S. M., Gil, M., Plane, J. M. C., and Saiz-Lopez, A.: Concurrent observations of atomic iodine, molecular iodine and ultrafine particles in a coastal environment, Atmos. Chem. Phys., 11, 2545-2555, https://doi.org/10.5194/acp-11-2545-2011, 2011.

McFiggans, G., Bale, C. S. E., Ball, S. M., Beames, J. M., Bloss, W. J., Carpenter, L. J., Dorsey, J., Dunk, R., Flynn, M. J., Furneaux, K. L., Gallagher, M. W., Heard, D. E., Hollingsworth, A. M., Hornsby, K., Ingham, T., Jones, C. E., Jones, R. L., Kramer, L. J., Langridge, J. M., Leblanc, C., LeCrane, J. P., Lee, J. D., Leigh, R. J., Longley, I., Mahajan, A. S., Monks, P. S., Oetjen, H., Orr-Ewing, A. J., Plane, J. M. C., Potin, P., Shillings, A. J. L., Thomas, F., von Glasow, R., Wada, R., Whalley, L. K., and Whitehead, J. D.: Iodine-mediated coastal particle formation: an overview of the Reactive Halogens in the Marine Boundary Layer (RHaMBLe) Roscoff coastal study, Atmos. Chem. Phys., 10, 2975-2999, https://doi.org/10.5194/acp-10-2975-2010, 2010.

McGrath, M. J., Olenius, T., Ortega, I. K., Loukonen, V., Paasonen, P., Kurten, T., Kulmala, M., and Vehkamaki, H.: Atmospheric Cluster Dynamics Code: a flexible method for solution of the birth-death equations, Atmos. Chem. Phys., 12, 2345-2355, https://doi.org/10.5194/acp-12-2345-2012, 2012.

Muller, C., Iinuma, Y., Karstensen, J., van Pinxteren, D., Lehmann, S., Gnauk, T., and Herrmann, H.: Seasonal variation of aliphatic amines in marine sub-micrometer particles at the Cape Verde islands, Atmos. Chem. Phys., 9, 9587-9597, https://doi.org/10.5194/acp-9-9587-2009, 2009.

Murphy, D. M. and Ravishankara, A. R.: Trends and patterns in the contributions to cumulative radiative forcing from different regions of the world, Proc. Natl. Acad. Sci. U. S. A., 115, 13192-13197, https://doi.org/10.1073/pnas.1813951115, 2018.

Ning, A., Liu, L., Zhang, S. B., Yu, F. Q., Du, L., Ge, M. F., and Zhang, X. H.: The critical role of dimethylamine in the rapid formation of iodic acid particles in marine areas, NPJ Clim. Atmos. Sci., 5, https://doi.org/10.1038/s41612-022-00316-9, 2022.

O'Dowd, C. D. and De Leeuw, G.: Marine aerosol production: a review of the current knowledge, Philos. Trans. R. Soc., A, 365, 1753-1774, https://doi.org/10.1098/rsta.2007.2043, 2007.

O'Dowd, C. D., Jimenez, J. L., Bahreini, R., Flagan, R. C., Seinfeld, J. H., Hameri, K., Pirjola, L., Kulmala, M., Jennings, S. G., and Hoffmann, T.: Marine aerosol formation from biogenic iodine emissions, Nature, 417, 632-636, https://doi.org/10.1038/nature00775, 2002a.

O'Dowd, C. D., Hameri, K., Makela, J., Vakeva, M., Aalto, P., de Leeuw, G., Kunz, G. J., Becker, E., Hansson, H. C., Allen, A. G., Harrison, R. M., Berresheim, H., Geever, M., Jennings, S. G., and Kulmala, M.: Coastal new particle formation: Environmental conditions and aerosol physicochemical characteristics during nucleation bursts, J. Geophys. Res.: Atmos., 107, https://doi.org/10.1029/2000jd000206, 2002b.

O'Dowd, C. D., Hämeri, K., Mäkelä, J. M., Pirjola, L., Kulmala, M., Jennings, S. G., Berresheim, H., Hansson, H.-C., de Leeuw, G., Kunz, G. J., Allen, A. G., Hewitt, C. N., Jackson, A., Viisanen, Y., and Hoffmann, T.: A dedicated study of new particle formation and fate in the coastal Environment (PARFORCE): Overview of objectives and achievements, J. Geophys. Res.: Atmos., 107, 1-16, https://doi.org/10.1029/2001jd000555, 2002c.

Peterson, K. A.: Systematically convergent basis sets with relativistic pseudopotentials. I. Correlation consistent basis sets for the post-d group 13–15 elements, J. Chem. Phys., 119, 11099-11112, https://doi.org/10.1063/1.1622923, 2003.

Pope, C. A., III and Dockery, D. W.: Health effects of fine particulate air pollution: lines that connect, J. Air Waste Manage. Assoc., 56, 709-742, https://doi.org/10.1080/10473289.2006.10464485, 2006.

Quelever, L. L. J., Dada, L., Asmi, E., Lampilahti, J., Chan, T., Ferrara, J. E., Copes, G. E., Perez-Fogwill, G., Barreira, L., Aurela, M., Worsnop, D. R., Jokinen, T., and Sipila, M.: Investigation of new particle formation mechanisms and aerosol processes at Marambio Station, Antarctic Peninsula, Atmos. Chem. Phys., 22, 8417-8437, https://doi.org/10.5194/acp-22-8417-2022, 2022.

Rappe, A. K., Casewit, C. J., Colwell, K. S., Goddard, W. A., and Skiff, W. M.: UFF, a full periodic-table force-field for molecular mechanics and molecular-dynamics simulations, J. Am. Chem. Soc., 114, 10024-10035,

https://doi.org/10.5194/egusphere-2023-1774
Preprint. Discussion started: 17 October 2023

https://doi.org/10.1021/ja00051a040, 1992.

Rong, H., Liu, J., Zhang, Y., Du, L., Zhang, X., and Li, Z.: Nucleation mechanisms of iodic acid in clean and polluted coastal regions, Chemosphere, 253, 126743, https://doi.org/10.1016/j.chemosphere.2020.126743, 2020.

Shampine, L. and Reichelt, M.: The MATLAB ODE suite. SIAM J. Sci. Comput. 18, 1–22, 1997.

Sipila, M., Sarnela, N., Jokinen, T., Henschel, H., Junninen, H., Kontkanen, J., Richters, S., Kangasluoma, J., Franchin, A., Perakyla, O., Rissanen, M. P., Ehn, M., Vehkamaki, H., Kurten, T., Berndt, T., Petaja, T., Worsnop, D., Ceburnis, D., Kerminen, V. M., Kulmala, M., and O'Dowd, C.: Molecular-scale evidence of aerosol particle formation via sequential addition of HIO3, Nature, 537, 532-534, https://doi.org/10.1038/nature19314, 2016.

Stewart, J. J.: Stewart Computational Chemistry, Colorado Springs, CO, USA, MOPAC 2016, Stewart Computational Chemistry, Colorado Springs, CO, USA, 2016.

Stewart, J. J. P.: Optimization of parameters for semiempirical methods VI: more modifications to the NDDO approximations and re-optimization of parameters, J. Mol. Model., 19, 1-32, https://doi.org/10.1007/s00894-012-1667-x, 2013.

Vanneste, A., Duce, R. A., and Lee, C.: Methylamines in the marine atmosphere, Geophys. Res. Lett., 14, 711-714, https://doi.org/10.1029/GL014i007p00711, 1987.

Xia, D. M., Chen, J. W., Yu, H., Xie, H. B., Wang, Y., Wang, Z. Y., Xu, T., and Allen, D. T.: Formation mechanisms of iodine-ammonia clusters in polluted coastal areas unveiled by thermodynamics and kinetic simulations, Environ. Sci. Technol., 54, 9235-9242, https://doi.org/10.1021/acs.est.9b07476, 2020.

Yang, Y., Weaver, M. N., and Merz, K. M.: Assessment of the "6-31+G**+LANL2DZ" mixed basis set coupled with density functional theory methods and the effective core potential: Prediction of heats of formation and ionization potentials for first-row-transition-metal complexes, J. Phys. Chem. A, 113, 9843-9851, https://doi.org/10.1021/jp807643p, 2009.

Yao, L., Garmash, O., Bianchi, F., Zheng, J., Yan, C., Kontkanen, J., Junninen, H., Mazon, S. B., Ehn, M., Paasonen, P., Sipila, M., Wang, M. Y., Wang, X. K., Xiao, S., Chen, H. F., Lu, Y. Q., Zhang, B. W., Wang, D. F., Fu, Q. Y., Geng, F. H., Li, L., Wang, H. L., Qiao, L. P., Yang, X., Chen, J. M., Kerminen, V. M., Petaja, T., Worsnop, D. R., Kulmala, M., and Wang, L.: Atmospheric new particle formation from sulfuric acid and amines in a Chinese megacity, Science, 361, 278-281, https://doi.org/10.1126/science.aao4839, 2018.

Yu, F. and Luo, G.: Modeling of gaseous methylamines in the global atmosphere: impacts of oxidation and aerosol uptake, Atmos. Chem. Phys., 14, 12455-12464, https://doi.org/10.5194/acp-14-12455-2014, 2014.

Yu, H., Ren, L. L., Huan, X. P., Xie, M. J., He, J., and Xiao, H.: Iodine speciation and size distribution in ambient aerosols at a coastal new particle formation hotspot in China, Atmos. Chem. Phys., 19, 4025-4039, https://doi.org/10.5194/acp-19-4025-2019, 2019.

Zhang, J. and Dolg, M.: ABCluster: The artificial bee colony algorithm for cluster global optimization, Phys. Chem. Chem. Phys., 17, 24173-24181, https://doi.org/10.1039/c5cp04060d, 2015.

Zhang, R., Khalizov, A., Wang, L., Hu, M., and Xu, W.: Nucleation and growth of nanoparticles in the atmosphere, Chem. Rev., 112, 1957-2011, https://doi.org/10.1021/cr2001756, 2012.

Zhang, R. J., Xie, H. B., Ma, F. F., Chen, J. W., Iyer, S., Simon, M., Heinritzi, M., Shen, J. L., Tham, Y. J., Kurten, T., Worsnop, D. R., Kirkby, J., Curtius, J., Sipila, M., Kulmala, M., and He, X. C.: Critical role of iodous acid in neutral iodine oxoacid nucleation, Environ. Sci. Technol., https://doi.org/10.1021/acs.est.2c04328, 2022a.

Zhang, R. Y.: Getting to the critical nucleus of aerosol formation, Science, 328, 1366-1367, https://doi.org/10.1126/science.1189732, 2010.

Zhang, S. B., Li, S. N., Ning, A., Liu, L., and Zhang, X. H.: Iodous acid - a more efficient nucleation precursor than iodic acid, Phys. Chem. Chem. Phys., 24, 13651-13660, https://doi.org/10.1039/d2cp00302c, 2022b.